Acc #726579
DP-MS-71-2

FORCED CONVECTION SUBCOOLED CRITICAL HEAT FLUX
PART II. HEATER MATERIAL EFFECT: ALUMINUM VERSUS STAINLESS STEEL

by

D. H. Knoebel, S. D. Harris, and B. Crain, Jr.

Savannah River Laboratory
E. I. du Pont de Nemours & Co.
Aiken, South Carolina 29801

and

R. M. Biderman

Chemical Engineering Research Laboratories
Columbia University
New York, New York 10027

For Presentation at the

12th National Heat Transfer Conference
Tulsa, Oklahoma

August 15-18, 1971

And for Publication in

Transactions of the ASME - Journal of Heat Transfer Series C

2/22/71

This document was prepared in conjunction with work accomplished under Contract No. DE-AC09-96SR18500 with the U. S. Department of Energy.

FORCED CONVECTION SUBCOOLED CRITICAL HEAT FLUX
PART II. HEATER MATERIAL EFFECT: ALUMINUM VERSUS STAINLESS STEEL*

by

D. H. Knoebel, S. D. Harris, and B. Crain, Jr.

Savannah River Laboratory
E. I. du Pont de Nemours & Co.
Aiken, South Carolina 29801

and

R. M. Biderman

Chemical Engineering Research Laboratories
Columbia University
New York, New York 10027

ABSTRACT

Critical heat flux data and correlations are presented for aluminum surfaces with both light water (H_2O) and heavy water (D_2O) coolant. The critical heat flux for aluminum heaters was determined to be at least 20% higher than that for stainless steel at the same coolant velocity and subcooling. A brief discussion of possible mechanisms for the phenomenon is included.

* Part of the information contained in this article was developed during the course of work under Contract AT(07-2)-1 with the U. S. Atomic Energy Commission.

FORCED CONVECTION SUBCOOLED CRITICAL HEAT FLUX
PART II. HEATER MATERIAL EFFECT: ALUMINUM VERSUS STAINLESS STEEL*

by

D. H. Knoebel, S. D. Harris, and B. Crain, Jr.

Savannah River Laboratory
E. I. du Pont de Nemours & Co.
Aiken, South Carolina 29801

and

R. M. Biderman

Chemical Engineering Research Laboratories
Columbia University
New York, New York 10027

INTRODUCTION

The Savannah River Laboratory (SRL) has been engaged in studies to better define the critical heat fluxes for fuel assemblies used in the Savannah River Plant reactors. An earlier paper [1] described studies to determine the effect of D_2O coolant versus H_2O coolant on the critical heat flux. The critical heat flux for D_2O was determined to be 16% greater than that for H_2O at same coolant velocity and subcooling.

This paper presents critical heat fluxes obtained for aluminum heaters and compares the results to those obtained with stainless steel heaters. An empirical critical heat flux correlation presented depends on both the coolant and heater physical properties. An analytical model was developed to study the dynamic interaction of internal heat conduction and heat transfer across the coolant heater interface during a burnout transient.

---

* Part of the information contained in this article was developed during the course of work under Contract AT(07-2)-1 with the U. S. Atomic Energy Commission.

SUMMARY

The critical heat flux for aluminum heaters is at least 20% higher than that for stainless steel at the same coolant conditions. This difference was determined by 60 tests at Columbia University. The empirical correlation presented earlier [1] was modified with an additional term to account for differences in heater material. The following equation predicts the critical heat flux for uniformly heated stainless steel and aluminum heaters and uniform cooling for both H_2O and D_2O with a standard deviation of 4.5%

$$\left.\frac{Q}{A}\right|_{Cr} = 11{,}100 \left(\frac{We}{Re}\right)_C^{0.567} \left(\frac{C_p\, T_{sub}}{\lambda}\right)_C^{0.767} \left(\frac{k}{\rho C_p}\right)_H^{0.077} \qquad (1)$$

This equation is valid for coolant velocities from 15 to 60 ft/sec. Subcoolings from 45 to 180°F, and pressures from 30 to 100 psia.

Heaters with 0.020-, 0.028- and 0.035-inch wall thickness were used. The data indicate an increase in burnout heat flux with wall thickness (Figure 2); however, sufficient data are not available to verify the exact dependence. The increase in critical heat flux for aluminum is attributed to the thermal properties of aluminum versus stainless steel and to the time scale associated with burnout with forced-convection subcooled coolant.

BACKGROUND

The effect of heater material on the critical heat flux has been investigated with pool boiling conditions [2,3]. Tests indicated that although stainless steel and copper had equivalent critical heat fluxes, critical heat fluxes for aluminum were up to 20% greater. Because the thermal properties of copper are much better than those of aluminum and because the critical heat fluxes for copper agree with those for stainless steel, the higher critical heat flux at pool boiling conditions for aluminum cannot be attributed to the thermal properties.

Previous work at SRL indicated that critical heat fluxes for aluminum with forced convection cooling were higher than those for stainless steel. These tests were limited by the power supply at SRL. In 1966, a program was begun at Columbia University to measure the burnout heat fluxes with aluminum surfaces over a broader range. Initial heater designs at Columbia University contained an indirectly heated aluminum tube two inches in diameter (stainless steel heater electrically insulated from an outer aluminum sheath). Thermal expansion and assembly problems limited operation to below heat fluxes of about 1.5×10^6 Btu/hr ft^2. Higher heat fluxes were subsequently obtained with direct resistance heating of aluminum heaters with 0.75- and 1.0-inch-diameter heaters.

EXPERIMENTAL EQUIPMENT

The Heat Transfer Facility of Columbia University has 3.5 megawatts of direct current power available from two motor generator sets. The generators are connected in parallel and can supply a maximum of 20,000 amperes at 175 volts. This power source was used to heat the simulated reactor fuel elements used in these experiments.

The test loop had a maximum pressure rating of 250 psig and consisted of two centrifugal pumps, three shell and tube heat exchangers, a deionizer, a piston pump to control pressure, connecting piping, and a housing section to accommodate test sections. The two pumps were connected in series and were capable of providing 200 gpm at 350 feet differential head. The loop piping was stainless steel, but aluminum and copper did contact the water as part of the test section.

The flow rate was measured by a Potter turbine flow meter, and the inlet and outlet temperatures to the test section were measured by iron-constantan thermocouples and a temperature sensor. The inlet and exit pressures were measured by Bourdon-tube pressure gauges, and the pressure drop across the heated length of a simulated fuel rod was measured with a U-tube manometer.

The heaters were constructed of Type 5052 aluminum drawn over ceramic spacers. The heaters were installed vertically with the cooling water flowing downward. All experiments were run with subcooled flow at the exit of the test section. All test sections had a heated length of 24 inches and an overall length of six feet. The heater formed the inner wall of the coolant annulus. The outer wall was constructed of aluminum spacers designed to give the desired equivalent diameter. The extension pieces which comprised the majority of the length of the test section were either Type 6061 aluminum, nickel 200, or electrolytic copper. The electrical connectors at the ends of the test section were silver-plated copper.

Thermal expansion of the test section was permitted by "O" ring seals on the top and bottom. Counterweighting the heavy bus connectors prevented large tensile or compressive forces on the test section, and also increased the reliability of the joints of the test section.

The concentricity of the heater tube in the annulus was maintained by three sets of spacer pins mounted in the wall of the outer annular surface. Three pins in each set were spaced at 120° intervals. The pins contacted the heater with a concave surface which matched the curvature of the heater tube. Asbestos phenolic pins were used. Six sets of three pins each were used in later tests to improve concentricity.

EXPERIMENTAL PROCEDURE

Tests were conducted at constant flow and exit bulk temperature. The inlet temperature was decreased as the power (heat flux) was increased to the point of burnout. Some test conditions were recorded as safe operating points to avoid heater destruction. (The low melting point of the aluminum and high power density made use of a burnout detector impractical). These points were normally in excess of the critical heat flux of stainless steel by more than 15%. When this condition was reached, the heat flux, subcooling, and velocity were recorded, and conditions were changed for the next test. Results for tests listed as safe operating points with the recorded heat flux more than 5% below equation (1) were not included. The tests with physical burnout during the first test on a heater with heat fluxes more than 10% below equation (1) were also discarded. The low values of critical heat flux were attributed to heater fabrication defects.

RESULTS

The critical heat flux results for aluminum heaters and H_2O coolant included 18 tests* with physical burnout, 22 tests with safe operating points with critical heat fluxes more than 20% greater than stainless steel at equivalent coolant conditions and 20 tests with safe operating points with

---

* All test results presented in this paper are available from the Technical Information Service, Savannah River Laboratory, Aiken, S. C. 29801.

critical heat fluxes between 15 and 20% greater than stainless steel heaters. These results were correlated by the following equation

$$\left.\frac{Q}{A}\right|_{Cr} = 188,000\ (1 + 0.0515\ V)(1 + 0.069\ T_{sub}) \qquad (2)$$

Deviations from the correlation ranged from -6.6% to +17% for heater thicknesses of 0.020, 0.028, and 0.035 inches.

Several tests were conducted with aluminum heaters and D_2O coolant. The observed critical heat fluxes are correlated by the following equation, which predicts critical heat fluxes 40% greater than for H_2O and stainless surfaces

$$\left.\frac{Q}{A}\right|_{Cr} = 218,000\ (1 + 0.0515\ V)(1 + 0.069\ T_{sub}) \qquad (3)$$

Data are shown in Figure 3 compared to equation (3) and verify the independent increase in critical heat flux of 20% for aluminum over stainless steel surfaces and of 16% for D_2O over H_2O coolant [1].

The critical heat flux data obtained at SRL [1] and Columbia University with stainless steel and aluminum heaters and H_2O and D_2O coolant are correlated by equation (1). The correlation uses two dimensionless groups dependent on physical properties of the coolant. These groups, ratio of the We and Re numbers and the group $(C_p\ T_{sub}/\lambda)$, were used previously to correlate H_2O and D_2O data [1]. The third group or the thermal diffusivity $(k/\rho C_p)_H$ is used to represent the effect of the heater material on burnout. The group is not dimensionless and is used to provide a means of including differences in heater materials.

Critical heat fluxes were also determined for aluminum-oxide-coated aluminum heaters. The oxide coatings were formed either by a commercial anodizing process or steam autoclaving at SRL. The anodized heaters obtained from the first vendor had a specified oxide thickness of 1 mil. After several tests the oxide was measured to be a minimum of 2.4 mils thick. The oxide layers formed by autoclaving at SRL were up to 0.60-mil thick, and the anodized heaters from a second vendor had a maximum oxide thickness of 1.4 mils. There were significant differences in the thermal conductivity of the oxides (0.4 to 0.7 Btu/hr ft °F). The thermal conductivities were calculated from the known oxide thickness, the heat flux at failure, an assumed surface temperature of 360°F, and the internal surface temperature equal to the melting point of aluminum at the time of failure. The oxide thickness was determined by metallographic sectioning and measurement of the oxide thickness on a 1000X photograph of the section.

Test sections that operated at heat fluxes corresponding to internal temperatures in excess of 1100°F failed by internal melting instead of local burnout. Internal melting was verified in several tests by an internal thermocouple. The results of these tests are summarized in Figure 4. The oxide did not directly affect the critical heat flux, but did limit the operating heat flux when the large temperature gradients across the oxide layer caused internal melting.

DISCUSSION

The data indicating an effect of heater thickness of the critical heater flux are shown in Figure 2. Available data [2, 4] indicate that for very thin stainless steel heaters the critical heat flux is a function of heater thickness. For stainless steel this effect disappears at a thickness of 0.004 inch. Because of the factor of 12 difference in thermal conductivities, the critical heat flux for aluminum would approach an asymptotic value at about 0.050 inches which is verified by the trend shown in Figure 2.

In an attempt to understand the increased critical heat fluxes for aluminum versus stainless steel, an analytical computer model was developed. The model accounted for internal conduction and used surface heat transfer coefficients as a function of surface temperature. Burnout was initiated on the surface by decreasing the heat transfer coefficient at a local area to one-tenth the steady state value. This reduction represents placement of a vapor film on the surface. The heat transfer coefficient was held constant for some fixed time and was then allowed to follow the temperature dependence model. The surface then either recovered or melted. The time which represented the point between recovery or melting was a function of hydrodynamic conditions. This dynamic model did indicate that stainless steel should not have as high a critical heat flux as aluminum, but could not indicate magnitudes. The results of this theoretical study indicated that the difference was due to the time scale of burnout and the finning ability of that portion of the heater with temperatures below the Leidenfrost point. Note that a heater material effect based on thermal properties would not be applicable at pool boiling conditions where the vapor films are large, and the buoyancy forces and vapor residence times are controlling. Theoretical studies of burnout phenomena are continuing.

It should be noted that the equations presented herein are applicable only to ideal surfaces. Preliminary studies at SRL to determine the effect of a 60-mil spacer rib contacting an aluminum heater indicate as much as a 20% reduction in the critical heat flux predicted by the ideal correlations.

REFERENCES

1. Knoebel, D. H., Harris, S. D., and Biderman, R. M., "Forced Convection Subcooled Critical Heat Flux Part I. Effect of Coolant: D_2O versus H_2O," submitted for publication in *ASME Journal of Heat Transfer Series C* (1971).
2. Tachibana, F., Akiyama, M., and Kawamura, H., "Non-Hydrodynamic Aspects of Pool Boiling Burnout," *Journal of Nuclear Science and Technology 4*, 121 (1967).
3. Averin, E. K., *Izv. Acad. Nauk. SSSR, Otdel, Tekh. Nauk. 3*, 116 (1954); AERE-LIB/Trans 562, Harwell, Berkshire, England (1955).
4. Bernath, L., "A Theory of Local-Boiling Burnout and Its Application to Existing Data," *Chemical Engineering Progress Symposium Series*, Vol. 56, No. 30, 95 (1960).

PW:sce

NOMENCLATURE

$\left.\frac{Q}{A}\right|_{Cr}$ = critical heat flux, Btu/hr ft^2

$\frac{We}{Re}$ = ratio of the Weber number to the Reynolds number, $\mu V/\sigma g_c$

We = Weber number evaluated at film temperature, $\frac{V^2 D\rho}{\sigma g_c}$

Re = Reynolds number evaluated at film temperature, $\frac{V\rho D}{\mu}$

T_{film} = film temperature, °F; $\frac{T_{sat} + T_{bulk}}{2}$

T_{sub} = subcooling, °F; $T_{sat} - T_{bulk}$

T_{sat} = saturation temperature, °F

T_{bulk} = bulk coolant temperature, °F

D = bubble diameter on heater surface, ft

V = velocity, ft/sec

g_c = gravitational constant, lb_m ft/lb_f sec^2

C_p = specific heat capacity, Btu/lb_m °F

k = thermal conductivity, Btu ft/hr ft^2 °F

μ = viscosity at film temperature, lb_m/ft sec

σ = surface tension, lb_f/ft

λ = heat of vaporization at saturation temperature, Btu/lb_m

ρ = density, lb_m/ft^3

Subscripts: C = coolant

H = heater

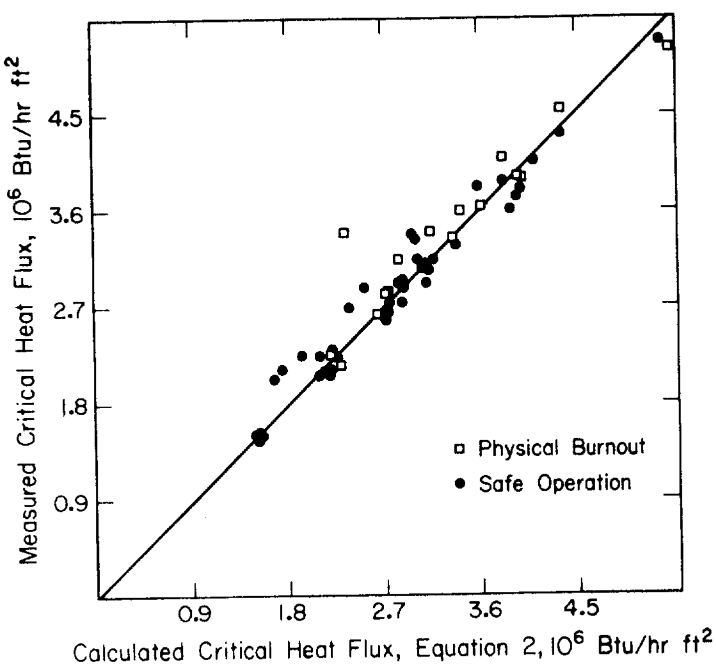

FIG. 1 CRITICAL HEAT FLUX RESULTS FOR ALUMINUM HEATERS AND H_2O COOLANT

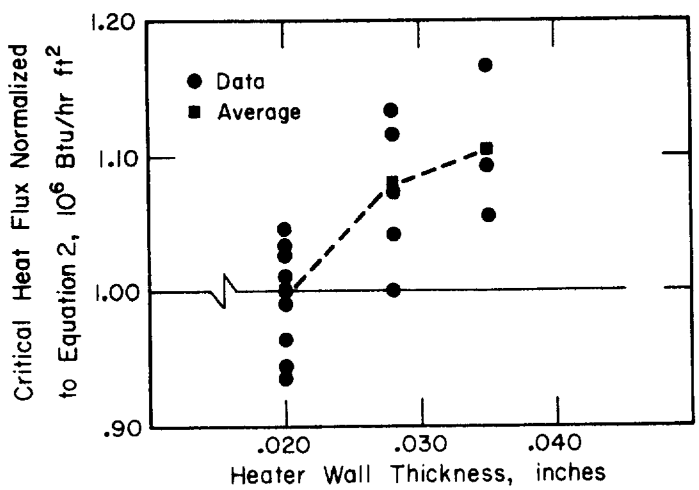

FIG. 2 EFFECT OF ALUMINUM HEATER THICKNESS ON THE CRITICAL HEAT FLUX

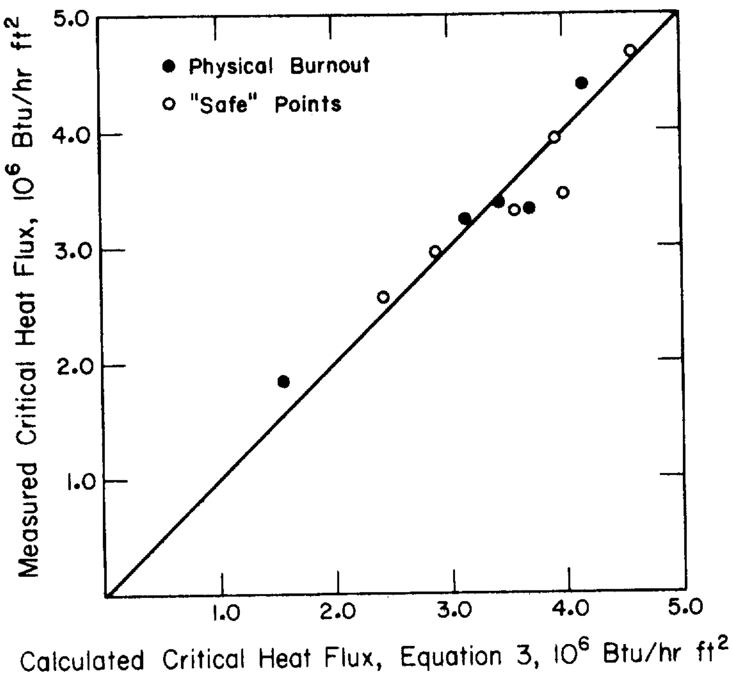

FIG. 3 CRITICAL HEAT FLUX WITH ALUMINUM HEATERS AND D_2O COOLANT

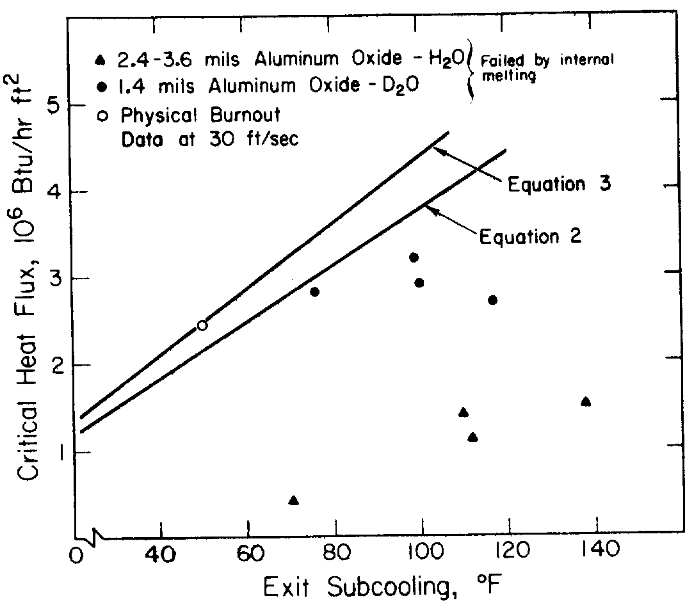

FIG. 4 EFFECT OF ALUMINUM OXIDE ON THE CRITICAL HEAT FLUX